

Letter to the editor

The ionospheric response during an interval of Pc5 ULF wave activity

M. Lester, J. A. Davies, T. K. Yeoman

Department of Physics and Astronomy, University of Leicester, Leicester, LE1 7RH, UK

Received: 21 June 1999 / Revised: 29 September 1999 / Accepted: 4 October 1999

Abstract. A preliminary analysis of Pc5, ULF wave activity observed with the IMAGE magnetometer array and the EISCAT UHF radar in the post midnight sector indicates that such waves can be caused by the modulation of the ionospheric conductivity as well as the wave electric field. An observed Pc5 pulsation is divided into three separate intervals based upon the EISCAT data. In the first and third, the Pc5 waves are observed only in the measured electron density between 90 and 112 km and maxima in the electron density at these altitudes are attributed to pulsed precipitation of electrons with energies up to 40 keV which result in the height integrated Hall conductivity being pulsed between 10 and 50 S. In the second interval, the Pc5 wave is observed in the F-region ion temperature, electron density and electron temperature but not in the D and E region electron densities. The analysis suggests that the wave during this interval is a coupled Alfvén and compressional mode.

Key words: Ionosphere (electric fields and currents) – Magnetospheric physics (magnetosphere–ionosphere interaction; MHD waves and instabilities).

1 Introduction

Observations of ULF waves by coherent radars such as STARE and SABRE are many (e.g. Walker *et al.*, 1979; Allan *et al.*, 1982; Yeoman *et al.*, 1990). From such observations, the electric field of the wave in the ionosphere could be measured for the first time (Walker *et al.*, 1979). Observations of waves with large azimuthal wave numbers, previously difficult to observe with ground based magnetometers, could also be made with these radars (Allan *et al.*, 1982). Furthermore, a method

for identifying the “compressiveness” of ULF waves was discussed by Yeoman *et al.* (1990). There are, however, few simultaneous observations of the variations in the ionospheric electron density, electron temperature and ion temperature during ULF wave activity (Doupnik *et al.*, 1977; Crowley *et al.*, 1985, 1987; Lathuillere *et al.*, 1986; Buchert *et al.*, 1999). Such observations are important to determine the ULF wave mode and the nature of the damping mechanism for ULF waves amongst other things. In this letter we present a preliminary analysis of observations by EISCAT during ULF waves in the interval 0200–0500 UT on April 21, 1993.

2 Magnetometer data

Band-pass filtered data, between 20 and 500 s, from four stations of the IMAGE array, Tromsø, Kilpisjärvi, Masi and Kevo, for the interval of interest are given in Fig. 1. Between 0230 and 0450 UT there appears to be a single Pc5 ULF wave, which is composed of several different wave packets, all of a similar frequency. The interval can be divided into three distinct parts (see also later), between 0230 and 0315 UT, 0315–0410 UT and 0410–0500 UT. The *Y*, geographic east-west, component (Fig. 1b) is the strongest component in the first interval, while the *X*, geographic north-south, (Fig. 1a) and *Y* components are comparable during the second interval and the *X* component is the largest in the third interval. Spectral analysis of the data from all IMAGE stations indicates that the dominant frequency in both *X* and *Y* components is 4.8 mHz, 5.2 mHz and 5.3 mHz in the first, second and third intervals, respectively. Note that the resolution of these frequencies is ± 0.4 mHz. Comparison of phase across the four stations in Fig. 1 provides an estimate of the azimuthal wave numbers, or *m* values. The outermost stations, TRO and KEV, have the smallest separation in latitude, 0.3° , thereby reducing any effects caused by latitudinal phase gradients, and are separated by 6.3° in longitude. Based upon these stations, the *X* and *Y* component *m* values for the

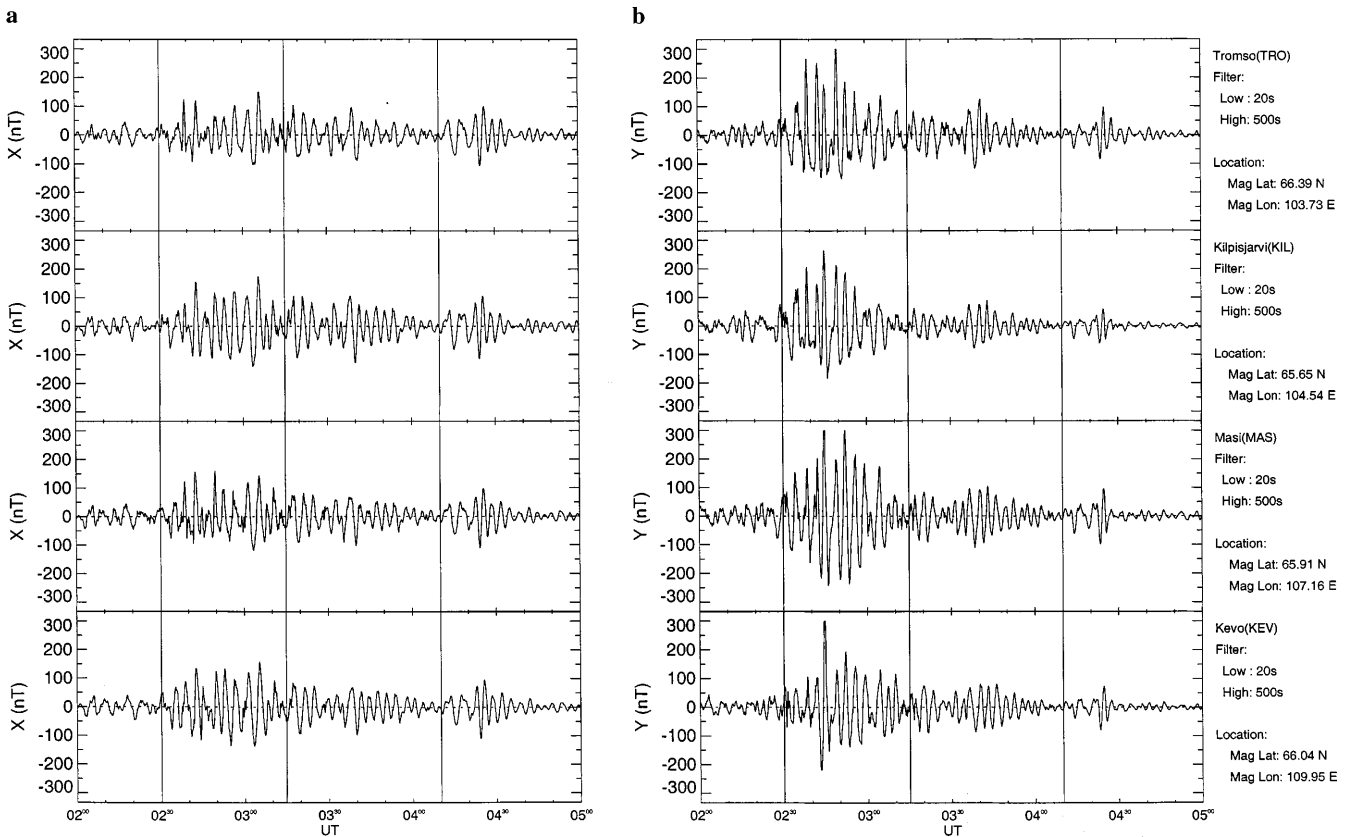


Fig. 1a, b. Band-pass filtered magnetometer data between 0200 and 0500 UT from Tromso (TRO), Kilpisjarvi (KIL), Masi (MAS) and Kevo (KEV). The filter bandwidth is 20 to 500 s. The X components

(north-south) are in **a** and the Y components (east-west) are in **b**. The vertical lines identify the three separate intervals of ULF wave activity as described in the text

dominant spectral component in each interval range between 13 and 18 (i.e. westward).

3 EISCAT data

During the interval, the EISCAT radar was operating in common mode CP-1-K which is a simple mode whereby the Tromsø UHF radar points in a direction which is approximately aligned along the magnetic field direction in the F-region. The two remote receiver beams intersect the Tromsø beam at an altitude of 278 km. The mode and experimental codes are described in detail elsewhere (e.g. Davies *et al.*, 1997). In this brief work we present both long pulse estimates of electron density and temperature and ion temperature at altitudes above 150 km, with a resolution of 22 km along the beam, and height integrated Hall and Pedersen conductivities derived from raw electron density measurements, or power profile, between 70 and 400 km at a resolution of 4.5 km. The Hall and Pedersen conductances have been calculated following the method outlined in Lester *et al.* (1996). The tristatic measurements of ion velocity at 278 km allow the calculation of the electric field.

Representative time series of electron density, N_e , electron temperature, T_e , ion temperature, T_i , at an altitude of ~ 212 km, the east-west, V_E , and north-south, V_N , components of the ion velocity at 278 km, and the

height integrated Hall conductivity, Σ_H , for the interval 0200 to 0500 UT are presented in Fig. 2a. The electron density, electron temperature, ion temperature and Σ_H are plotted with a 10 s integration, while the ion velocity data are plotted with a 20 s integration. Vertical lines are drawn to indicate the three separate intervals identified. The F-region measurements only respond to the wave activity between 0315 and 0410 UT, while there is periodic behaviour in Σ_H during both the first and third intervals but not the second.

In interval 1, 0230–0315 UT, N_e at 212 km is typically $1 \times 10^{11} \text{ m}^{-3}$. At this altitude T_e varies between 1200 and 1400 K and T_i between 800 and 1200 K. The larger ion temperatures are related to the enhanced ion velocities and are caused by ion frictional heating (e.g. Davies *et al.*, 1997). The lower E-region electron density (data not shown) is 10^{11} m^{-3} between 0210 and 0230 UT, but during the following 45 min it varies periodically between $5 \times 10^{10} \text{ m}^{-3}$ and $5 \times 10^{11} \text{ m}^{-3}$. A dominant spectral peak near 5.2 mHz is evident in the spectral analysis of the E-region electron density leads to the periodic variation in Σ_H between 10 and 50 S, shown in Fig. 2a, while the height integrated Pedersen conductivity, Σ_p , varies between 5 and 10 S.

During interval 2 there are clear periodic variations in F-region electron density, electron temperature and ion temperature. The maxima in N_e , about $3 \times 10^{11} \text{ m}^{-3}$, are the highest values at these altitudes

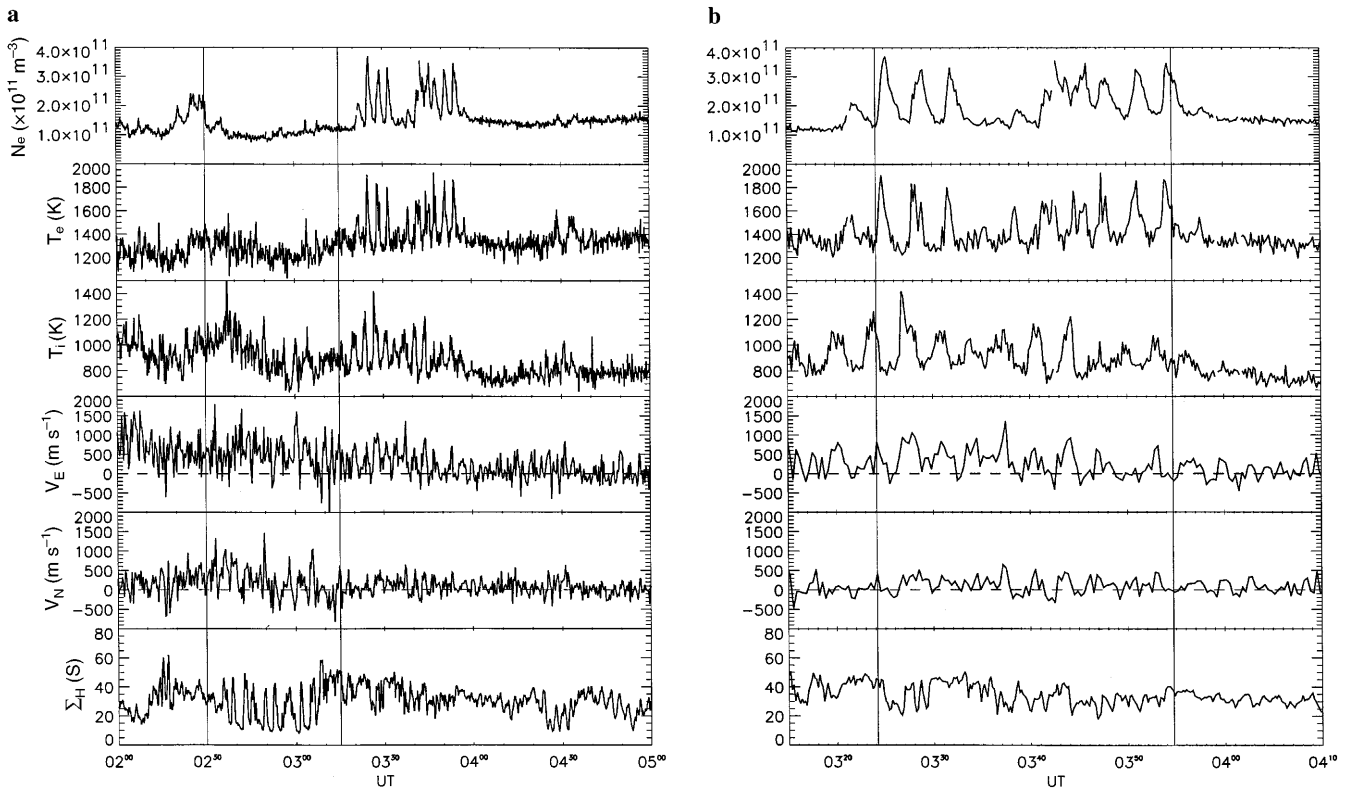


Fig. 2a, b. The EISCAT parameters, electron density at 212.5 km, electron temperature at 212.5 km, ion temperature at 212.5 km, the east-west component of the ion velocity at 278 km, the north-south component of the ion velocity at 278 km and the height integrated

conductivity Hall conductivity. **a** covers the time interval 0200 to 0500 UT and **b** the interval 0315 to 0410 UT. The *vertical lines* in **a** identify the three separate intervals of ULF wave activity as described in the text

during the whole interval. Similarly, the peak values in T_e of 1800 K also represent the largest values at this altitude during the interval. Variations in T_i are at least 200 K larger than the background values, and typically peak at 1200 K, while the variations in the ion velocity appear largest in the east-west component, with peak values of $+1.0 \text{ km s}^{-1}$, which means the ion velocity is enhanced in the eastward direction. There are no periodic variations in Σ_H , although the values are larger than at almost any other time during the whole interval. Spectral analysis of N_e , T_e , T_i , V_E , V_N and the magnitude of the ion velocity indicates a dominant spectral peak of 5.1 mHz in all parameters.

During the final wave packet observed by the magnetometer data, the F-region parameters are fairly constant throughout the interval with no sign of the periodicities seen earlier. There are, however, clear periodic variations in Σ_H between 0420 and 0500 UT with no similar variations in Σ_P . The dominant spectral peak in the E-region electron density is 5.3 mHz.

The EISCAT measurements during the second of the wave packets demonstrate the relative variations in the F-region ionospheric parameters during the ULF wave activity. Figure 2b is in the same format as Fig. 2a but covers the interval 0315 UT to 0410 UT. There are two separate packets of pulsed behaviour in electron density and temperature. Initially there are four peaks in N_e and T_e between 0320 UT and 0334 UT, and a further six pulses in the second packet. On the other hand,

T_i appears to be pulsed throughout the period up to 0400 UT.

The first signature of the wave activity occurs at 0319 UT when T_i increases from 800 K to more than 1000 K. The pulse of enhanced T_i lasts for approximately 120 s and is followed by an interval of unperturbed ion temperature. This behaviour continues and the ion temperature has the appearance of a square wave. During this pulse of enhanced ion temperature, N_e and T_e are low and become enhanced as T_i decreases. Normally T_e peaks just before or at the same time as N_e and also begins to decrease before N_e . In contrast to T_i , the pulses in N_e and T_e have rapid rise times to a peak value with subsequent slower decay times. A cross correlation analysis of the three time series indicates that the ion temperature and electron density are exactly 180° out of phase while the electron temperature leads the electron density by about 40° . This latter phase difference is a result of the decrease in electron temperature leading that in electron density.

4 Discussion

The Pc5 wave activity observed in the magnetometer data can be divided into three separate intervals as a result of the analysis of the EISCAT data. In the first and third intervals, the only response in the EISCAT observations is in the lower E-region and D-region

electron density, while in the second interval the response is seen in the F-region but not in the lower E- or D-regions. For the purpose of this work we discuss separately the wave activity in the first and second intervals.

A careful study of the electron density as a function of altitude during the first interval (data not shown) indicates that the wave occurs in the electron density measured between 90 km and 112 km altitude, with the largest variations in density at ~ 99 km. At this altitude the peak density is $5 \times 10^{11} \text{ m}^{-3}$, with a minimum density of $5 \times 10^{10} \text{ m}^{-3}$. The cause of such pulsed behaviour in electron density is most likely pulsed particle precipitation since such densities are higher than expected for this local time, ~ 0430 LT, in April. It is instructive to consider the energy of the particles which would cause such ionisation at these altitudes. For a monoenergetic, field-aligned beam of electrons of 20 keV the peak ionisation rate occurs near 100 km (Rees, 1989), while a beam of electrons of 40 keV has a peak ionisation rate near 90 km. A detailed inversion of the ionisation profile would provide a more accurate energy spectrum but is not attempted here. This variation in D-region and lower E-region densities leads to the conductance varying between 10 and 50 S.

Recently, Buchert *et al.* (1999) have reported observations of a ULF wave in the afternoon sector during which the conductance varied by a factor of 2. These authors concluded that the cause of the conductance variations was pulsed electron precipitation in the energy range 2–5 keV. The electrons which caused the conductance variations presented in Fig. 1 are of much higher energy than those reported by Buchert *et al.* (1999). The m value of the event discussed by Buchert and colleagues is 30, larger than that of the wave in Fig. 1, while the direction of phase propagation is westward for both events. However as the local time of the event discussed here is pre-dawn, a westward phase propagation is consistent with the wave being driven by the solar wind as it passes over the magnetopause and by ions drifting in the magnetosphere. Thus, it is not possible to distinguish between these two driving mechanisms, as in the case of Buchert *et al.* (1999). It is also worth noting that no significant solar or substorm activity took place at the time of either observation, although a substorm did occur a few hours before the case reported here.

Moving to interval two, the first point to discuss is the change in the E-region density. The density at 99.4 km varies between 2 and $5 \times 10^{11} \text{ m}^{-3}$, starting at the higher value and gradually decreasing, although not monotonically. Again this density is higher than expected at these altitudes at this local time and is also higher than the density at higher altitudes. For example, at 112 km the density has a maximum of $3 \times 10^{11} \text{ m}^{-3}$ and is always lower than the values at 99 km. Secondly, there is no clear signature in the E-region density of the ULF wave activity seen in the magnetometer data or in the F-region ionospheric parameters. As discussed already the likely cause of the enhanced D region and lower E region ionisation is

particle precipitation and on this occasion it appears to be more continuous, if variable, rather than pulsed. The high electron densities lead to values in Σ_H which vary between 20 and 50 S.

The phase relationships between N_e , T_e and T_i represent the other intriguing aspect of this interval. The simultaneous enhancements in electron density and temperature are likely to be caused by particle precipitation, while the ion temperature enhancements are caused by enhancements in the ion velocity, most easily seen in the eastward component (Fig. 2). The latter enhancements are possibly caused by the ULF wave electric field. Of the ULF wave modes, the Alfvén mode has a significant electric field in the ionosphere (e.g. Yeoman *et al.*, 1990). Observations by SABRE demonstrated that ULF waves are found to be increasingly compressional as the azimuthal wave number increased, at least up to a value of 12. The magnetometer observations discussed earlier indicate that the wave numbers are > 13 , suggesting that the wave observed during the second interval had a significant compressional component as well as an Alfvénic component. Furthermore, the wave frequency of 5.2 mHz during this interval is close to the expected resonant frequency for the latitude of Tromsø (e.g. Mathie *et al.*, 1999).

The high Σ_H indicates continuing precipitation of high energy particles which is not pulsed as in the first and third intervals. The particles causing the enhanced D and lower E-region electron densities are of much higher energy than those which are believed to be causing the enhancements in the F-region electron density and temperature. Why the higher energy part of the spectrum is not pulsed is unclear, however.

5 Conclusions

We report joint observations of Pc5 pulsations by the IMAGE magnetometer array and EISCAT. Such observations are rare, although with improvements to the receiver sensitivity at Tromsø we anticipate that more events will be observed. The interval of ULF wave activity examined here has two different responses in the ionosphere. In the first part of the interval, only enhancements in lower E region and D region electron densities are observed. We suggest these are caused by pulsed particle precipitation at energies of order 20–40 keV. Furthermore, the ground magnetic signature may simply be a response to the changing Hall conductivity. In the second interval a complicated phase relationship between the ion temperature and electron density and temperature exists. There are two processes occurring, one associated with the wave electric field and the other with the pulsed precipitation of low energy particles. The joint observations of the ULF wave electric field and high wave number indicates that the wave consists of both Alfvén and fast modes. Simultaneously, there continues to be precipitation of high energy particles, 20–40 keV, in order to maintain the high Hall conductance. The preliminary analysis under-

taken here cannot distinguish whether this is solely a temporal variation or solely a spatial variation. The interval does clearly respond in two different ways during the period of ULF wave activity, without any clear difference in the ground magnetic signatures at the time. Further detailed modelling and analysis of this event is required and will be presented in a future study.

Acknowledgements. EISCAT is funded by the research agencies of Finland, France, Germany, Japan, Norway, Sweden and the United Kingdom. The IMAGE magnetometer data used in this work were collected as a German-Finnish-Norwegian-Polish project conducted by the Technical University of Braunschweig, Germany.

The Editor-in-chief thanks F. Menk for his help in evaluating this paper.

References

- Allan, W., E. M. Poulter, and E. Nielsen, STARE observations of a Pc5 pulsation with large azimuthal wave numbers, *J. Geophys. Res.*, **87**, 6163–6172, 1982.
- Buchert, S. C., R. Fujii, and K.-H. Glassmeier, Ionospheric conductivity modulation in ULF pulsations, *J. Geophys. Res.*, **104**, 10 119–10 133, 1999.
- Crowley, G., N. Wade, J. A. Waldock, T. R. Robinson, and T. B. Jones, High time-resolution observations of periodic frictional heating associated with a Pc5 micropulsation, *Nature*, **316**, 528, 1985.
- Crowley, G., W. J. Hughes, and T. B. Jones, Observational evidence of cavity modes in the Earth's magnetosphere, *J. Geophys. Res.*, **92**, 12 233–12 240, 1987.
- Davies, J. A., M. Lester, and I. W. McCreath, A statistical study of ion frictional heating observed by EISCAT, *Ann. Geophysicae.*, **15**, 1399–1411, 1997.
- Doupnik, J. R., P. M. Banks, and A. Brekke, Incoherent scatter radar observations during three sudden commencements and a Pc5 event on August 4, 1972, *J. Geophys. Res.*, **82**, 499–514, 1977.
- Lathuillere, C., F. Glangeaud, and Z. Y. Zhao, Ionospheric ion heating by ULF Pc5 magnetic pulsations, *J. Geophys. Res.*, **91**, 1619–1626, 1986.
- Lester, M., J. A. Davies, and T. S. Virdi, High latitude Hall and Pedersen conductances during substorm activity in the SUN-DIAL-ATLAS Campaign, *J. Geophys. Res.*, **101**, 26 719–26 728, 1996.
- Mathie, R. A., F. W. Menk, I. R. Mann, and D. Orr, Discrete field line resonances and the Alfvén continuum in the outer magnetosphere, *Geophys. Res. Lett.*, **26**, 659–662, 1999.
- Rees, M. H., *Physics and chemistry of the upper atmosphere*, Cambridge University Press, Cambridge, UK, 1989.
- Walker, A. D. M., R. A. Greenwald, W. F. Stuart, and C. A. Green, STARE auroral radar observations of Pc5 geomagnetic pulsations, *J. Geophys. Res.*, **84**, 3373–3308, 1979.
- Yeoman, T. K., M. Lester, D. Orr, and H. Lühr, Ionospheric boundary conditions of hydromagnetic waves: the dependence on azimuthal wave number and a case study, *Planet. Space Sci.*, **38**, 1315–1325, 1990.